Available online at www.eccomasproceedia.org
Eccomas Proceedia COMPDYN (2023) 2249-2260

ECCOMAS
Proceedia

COMPDYN 2023
9th ECCOMAS Thematic Conference on
Computational Methods in Structural Dynamics and Earthquake Engineering
M. Papadrakakis, M. Fragiadakis (eds.)
Athens, Greece, 12-14 June 2023

ADVANCED MODELLING AND RISK ANALYSIS OF A RC BUILDING EQUIPPED WITH ENERGY DISSIPATION DEVICES DESIGNED BY THE ITALIAN SEISMIC CODE

E. Bruschi[1], V. Quaglini[1], M. Furinghetti[2], and A. Pavese[2]

[1] Politecnico di Milano
Piazza Leonardo da Vinci 32, 20133 Milan, Italy
e-mail: {eleonora.bruschi, virginio.quaglini}@polimi.it

[2] University of Pavia
Via Ferrata 3, 27100 Pavia, Italy
{marco.furinghetti, a.pavese}@unipv.it

Abstract

Among the modern techniques envisaged to improve the seismic performance of structures there is energy dissipation, which consists in dissipating part of the seismic input energy by means of special devices, i.e., the dampers, which are not part of the structural frame supporting gravity loads. Energy dissipation systems are typically designed to provide structural safety at the Life Safety ultimate limit state, but at the same time they are required, according to current Seismic Codes, to resist to earthquakes of higher intensity, corresponding to the case of Non-Collapse Limit State. However, the literature is missing of studies about the behavior of structures equipped with damped braces under collapse condition. In this contribution, an existing RC structure is retrofitted for a high seismicity area using steel braces equipped with hysteretic devices. Non-linear dynamic analyses are carried out considering two sets of bidirectional natural ground motions, correspondent to the Life Safety Limit State (LLS) and Non-Collapse Limit State (CLS). The aim of the research is to identify critical aspects of the retrofit design and to provide the basis for the computations of the implicit risk of the seismic collapse of the retrofitted structure and of the local failure of the dampers.

Keywords: Energy dissipation, Hysteretic Dampers, Non-linear Dynamic Analysis, Implicit Risk.

ISSN:2623-3347 Published by Eccomas Proceedia.
Peer-review under responsibility of the organizing committee of COMPDYN 2023.
doi: 10.7712/120123.10557.20312

1 INTRODUCTION

The seismic rehabilitation of existing buildings is aimed at preventing structural damage, increasing life-safety and achieving a desired level of performance [1]. Both energy dissipation and base isolation systems have demonstrated to be effective in improving the seismic performance of buildings, protecting either the structure and its content [2]-[7]. Generally, these systems are designed to be engaged during the design earthquake and to satisfy the structural safety requirement at the ultimate limit state to protect the life of the occupants. However, the Seismic Codes (e.g., [8], [9]) require that these systems are also able to resist earthquakes of higher intensity, which correspond to the non-collapse limit state. While the behavior of structures equipped with either dampers or isolators under design conditions and the effectiveness of different systems have been widely investigated by several authors [10]-[19], there is a lack of information about their behavior under collapse conditions. It is worth mentioning that some studies and experimental investigations about isolated structures behavior under collapse conditions and for high seismic intensities are available in the literature [20]-[24]; on the other hand, to the Authors' knowledge, this kind of studies is missing for structures equipped with energy dissipation devices.

The present study aims to identify critical aspects of the effectiveness of energy dissipation system in limiting building damage for high seismic intensities and to provide the basis for the implicit risk of damage assessment and global collapse considering over-stroke displacement of the dampers. The work is part of a larger investigation aimed at developing the second generation of Eurocodes, in which new partial safety factors are introduced consistently for the design of new structures as well as for the assessment and retrofitting of existing ones [25].

This contribution describes part of the research activity carried out on an existing reinforced concrete (RC) frame structure retrofitted for a high seismicity area according to the Italian seismic code (NTC-18) [8] by means of steel braces equipped with hysteretic devices characterized by different ductility levels. The European standard on anti-seismic devices EN15129 [26], which is compulsory in Europe for the CE Marking, requires that the hysteretic dampers shall be able to sustain a maximum displacement $\gamma_x \cdot \gamma_b \cdot d_{bd}$, where d_{bd} is the design seismic displacement of the damper, γ_x is the reliability factor according to the Eurocode with a recommended value of 1.2, and γ_b is and amplification factor, whose value shall be not less than 1.1 according to [26]. In this work, the case-study building is retrofitted in order to guarantee the Immediate Occupancy structural performance level, i.e., the condition in which the structure, after the design earthquake, is immediately accessible as it retains its original strength and stiffness. Non-linear dynamic analyses are performed considering 7 bidirectional natural accelerograms for two different limit states, namely the Life safety Limit State (LLS) and the Non-Collapse Limit State (CLS), in order to verify the displacement capacity of the damper.

The structure of the present contribution will follow this scheme. In Chapter 2, the case-study structure is presented, while Chapter 3 describes the modelling choices in OpenSees [27], [28] for the building and the energy dissipation system. The retrofit design of the building is reported in Chapter 4, and the selection of the seismic input is shown in Chapter 5. The results of the non-linear analyses (pushover and time-histories) are eventually detailed in Chapter 6.

2 DESCRIPTION OF THE CASE-STUDY BUILDING

The case-study structure is a residential 6-story RC building, designed according to the NTC-18 [8], which provides a similar approach to the Eurocode 8 [9], for a moderate seismicity zone corresponding to the municipality of Pordenone, Italy [29], characterized by a PGA = 1.91 m/s^2 and soil type B. Sketches of the building, with the main dimensions in plan and in elevation, are shown in Figure 1. This building is characterized by square 50x50cm columns at the ground

level and at the first floor, and by square 40x40cm columns from the second to the last floor, Figure 1. This arrangement results in a variation of stiffness along the height of the building and different floor masses at each story. The longitudinal reinforcement of columns and beams is listed in Table 1; structural loads and additional design information are reported in reference [29].

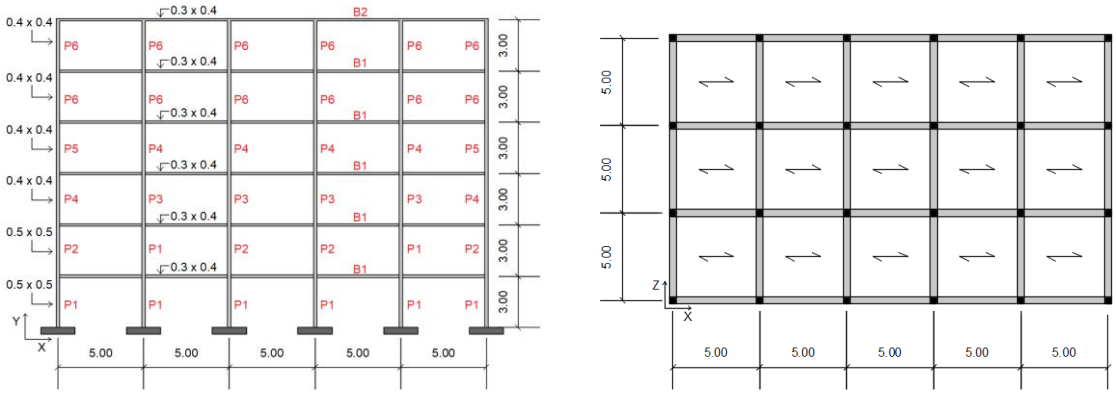

Figure 1: Elevation and plan view of the RC case-study structure.

ID	Longitudinal reinforcement (top + bottom bars)	Transverse reinforcement (stirrups dimension/spacing at beam-column joint)
P1	12ϕ18	ϕ12/5 cm
P2	12ϕ18	ϕ12/8 cm
P3	8ϕ18	ϕ12/5 cm
P4	8ϕ18	ϕ12/8 cm
P5	8ϕ18	ϕ12/10 cm
P6	8ϕ18	ϕ12/12.5 cm
B1	4 + 2ϕ16	ϕ8/8 cm
B2	3 + 2ϕ16	ϕ8/8 cm

Table 1: Cross-section details of beams and columns of the RC frame according to the nomenclature of Figure 1.

The structure is intended to fail in flexure, thus other failure mechanisms (such as shear failure of beams, columns or beam-column joints, bond slip and low-cycle fatigue, etc.) are out of the scope of the present work.

For the seismic upgrade of the structure, steel braces equipped with hysteretic dampers characterized by an elastic-perfectly plastic behavior are used.

3 NUMERICAL MODEL IN OPENSEES

Full 3-D numerical model of the structure is formulated within the OpenSees framework [27], [28], by following the references [30], [31]. The structural elements are modeled using the *forceBeamColumn* element object [32], in the form of the *beamWithHinges* element [28], assigning a linear elastic material behavior to the internal sub-element, whereas non-linearities can be activated only in the two external sub-elements. The length of these external regions, which corresponds to the plastic hinge length L_{pl}, is evaluated by applying the equation (A.9) of the Eurocode 8 [33], valid when a well-detailed confinement model of concrete is assumed. In these plastic regions, the concrete non-linear behavior is modelled through a fiber section model, where each steel bar corresponds to a single fiber using uniaxial Giuffre-Menegotto-Pinto constitutive law [34], equivalent to *Steel02* material model with isotropic strain hardening [35]. The strain-hardening ratio b is assumed equal to 0.005, as specified in reference [29]. The

parameters that control the transition from the elastic to the plastic branch are assigned as R_0 =18, C_{R1} = 0.925 and C_{R2} = 0.15 [28]. The concrete model is implemented using the library uniaxial material *Concrete04*, which is based on the model proposed by Popovics [36]; the properties of the core region of the sections are evaluated referring to Equations (A.6 – A.8) of the Eurocode 8 [33] and the tensile strength of concrete is neglected in both core and cover regions [37]. It is worth mentioning that the material properties of the building are evaluated disregarding the confidence factors [8], [33]. In order to account for concrete cracking, the interior elastic sub-element is characterized by an effective area moment of inertia I_{eq}, equal to 50% of the gross area moment of inertia I_g, according to the provisions of the Italian and the European norms [8], [9].

In all models, the masses of the structural members (beams, columns, and slabs) are concentrated at the center of mass of each floor; dead and live loads are uniformly distributed on each beam and have been calculated according to the tributary area concept; P-Delta effects are considered in the analyses, while bond slip and low-cycle fatigue effects are disregarded. The columns at the ground floor have fixed base supports, simulating rigid foundations. The damping of the frame is defined according to the Rayleigh method, as a function of the tangent stiffness matrix only, assuming 5% viscous damping ratio, to take into account the energy dissipation coming from infill panels and other non modelled non-structural components [30], [31]. The floor slabs are modelled as rigid diaphragms, by constraining the nodes belonging to the same floor to have the same displacement. An "axial buffer" [37] has been introduced in the FE model, through a *zeroLength* element object [38] characterized by a virtually zero axial stiffness and very high stiffnesses in shear and bending, placed between one end of each beam and the adjacent node belonging to the rigid diaphragm. This element works as an axial release to eliminate the fictitious axial force generated by the interaction between beam elements modelled with fiber sections and the rigid diaphragm [37].

The braces equipped with the hysteretic damper are modelled as truss elements [28] with an associated *uniaxialMaterial* model with elastic-perfectly plastic behavior [38].

4 RETROFIT OF THE CASE-STUDY STRUCTURE

The case-study building is upgraded for a high seismicity area, considering the seismic loads provided by the NTC-18 [8] for LLS, municipality of L'Aquila (Long 13° 23.9724', Lat 42° 21.033'), functional class cu = II, PGA = 4.062 m/s^2, soil type C and topographic factor T_2. Diagonal steel braces equipped with hysteretic devices are inserted in the facades, according to the layout shown in Figure 2 (4 units at each floor in both X and Z direction). These damped braces are characterized by ductility capacities μ_{DB} in the range 2÷6, in agreement with other studies [39]-[43]. In particular, the ductility capacity μ_{DB} and the correspondent energy dissipation capacity ξ_{DB} of the selected damped brace systems are reported in Table 2.

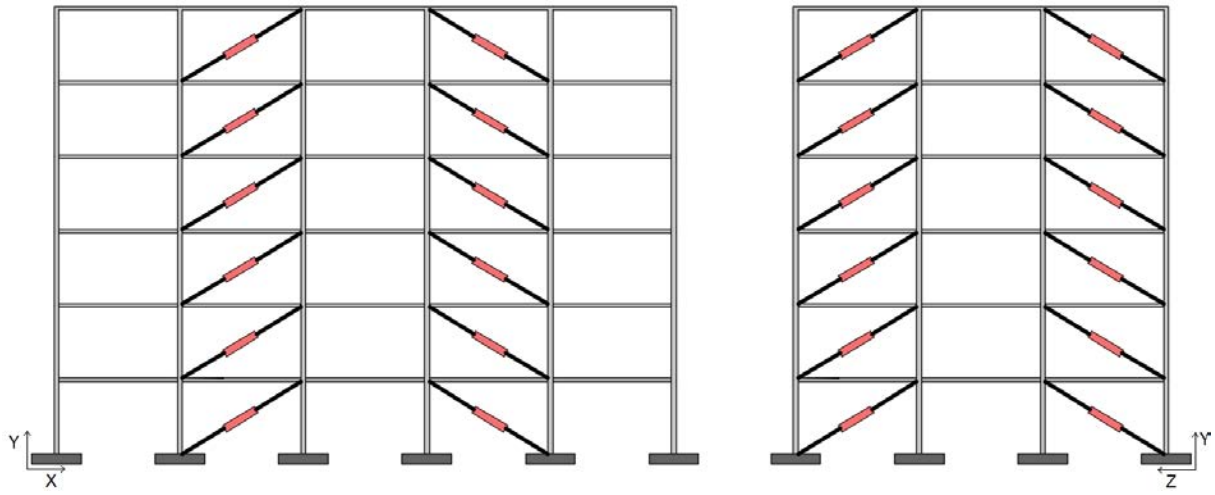

Figure 2: Diagonal layout of steel braces equipped with hysteretic dampers for case-study building.

μ_{DB} [-]	ξ_{DB} [%]
2	31.85
4	47.78
6	53.08

Table 2: Ductility factor μ_{DB} and energy dissipation capacity ξ_{DB} of the considered damped braces.

The dampers were sized for the Life safety Limit State (LLS) by applying the Direct Displacement-Based Design (DDBD) retrofit procedure developed by some Authors of this work [39]-[42]. In either direction of the building the target displacement d_p was selected as the ending point of the elastic part of the capacity curve, Figure 3. This performance level corresponds to the Immediate Occupancy performance level [3], which guarantees that the structure is immediately accessible after the design earthquake, since the strength and the stiffness of the structural elements are not compromised. Figure 3 shows the Single Degree Of Freedom (SDOF) capacity curves along X- and Z- directions with indications of the target displacement d^*_p.

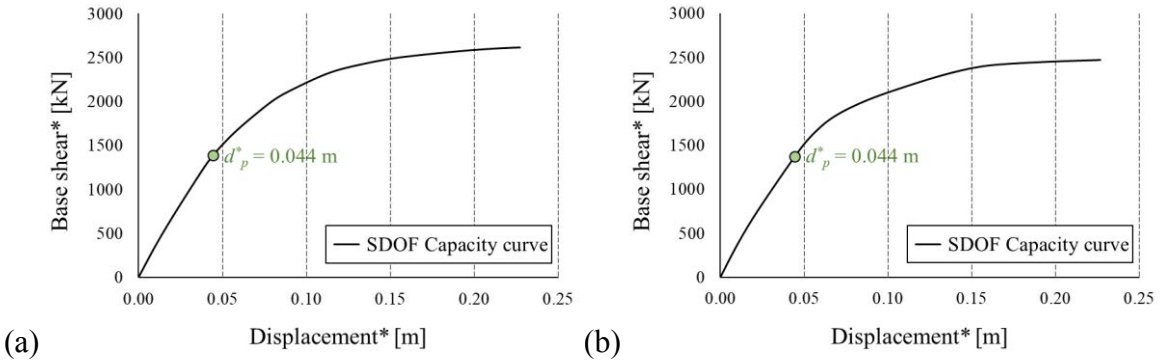

Figure 3: Capacity curves limit values of displacements d_p in X-direction (a) and Z-direction (b).

Table 3 reports the values of elastic stiffness K_{yi}^{DB} and axial force N_{yi}^{DB} of the damped brace units at each floor of the case-study structure provided from the design procedure for the assigned ductility factors μ_{DB} reported in Table 2.

Floor	$\mu_{DB} = 2$				$\mu_{DB} = 4$				$\mu_{DB} = 6$			
	X-direction		*Z-direcion*		*X-direction*		*Z-direction*		*X-direction*		*Z-direction*	
	K_{yi}^{DB} [kN/mm]	N_{yi}^{DB} [kN]	K_{yi}^{DB} [kN/mm]	N_{yi}^{DB} [kN]	K_{yi}^{DB} [kN/mm]	N_{yi}^{DB} [kN]	K_{yi}^{DB} [kN/mm]	N_{yi}^{DB} [kN]	K_{yi}^{DB} [kN/mm]	N_{yi}^{DB} [kN]	K_{yi}^{DB} [kN/mm]	N_{yi}^{DB} [kN]
1	471.4	1238.3	557.2	1339.0	568.5	811.6	580.9	811.6	780.1	742.5	797.1	742.4
2	242.6	1192.9	281.4	1290.9	292.5	781.9	293.4	782.4	401.5	715.3	402.6	715.7
3	180.3	1066.9	208.9	1155.6	217.5	699.3	217.8	700.4	298.4	639.8	298.9	640.7
4	174.5	850.2	200.8	922.0	210.4	557.3	209.3	558.8	288.7	509.8	287.2	511.2
5	170.9	555.1	195.6	602.6	206.1	363.8	203.9	365.2	282.8	332.8	279.8	334.1
6	133.5	207.6	149.6	225.7	161.0	136.1	156.0	136.8	220.9	124.5	214.0	125.2

Table 3: Properties of the damped braces for the investigated ductility factors μ_{DB}.

5 SEISMIC INPUT

Bidirectional non-linear dynamic analyses (BNLDA) are performed in accordance with the provisions of the Eurocode 8 [9] considering natural ground motions selected from the European Ground Motion Database [44] using the computer program REXEL [45]. The seismic inputs agree, in the interval of periods between 0.15 and 2.0 seconds, with the elastic spectra at 5% equivalent viscous damping ratio defined by the NTC-18 [8] for two different limit states, namely LLS and CLS, of an ordinary structure (functional class cu=II) with a nominal life V_n = 50 years, located in L'Aquila, soil type C, category T_2. The magnitude (Mw) of the seismic events was chosen within the interval [5 – 7], with an epicentral distance (Rep) in the range 0–30 km. Details of the input ground motions are provided in Figure 4 and Table 4 and Table 5.

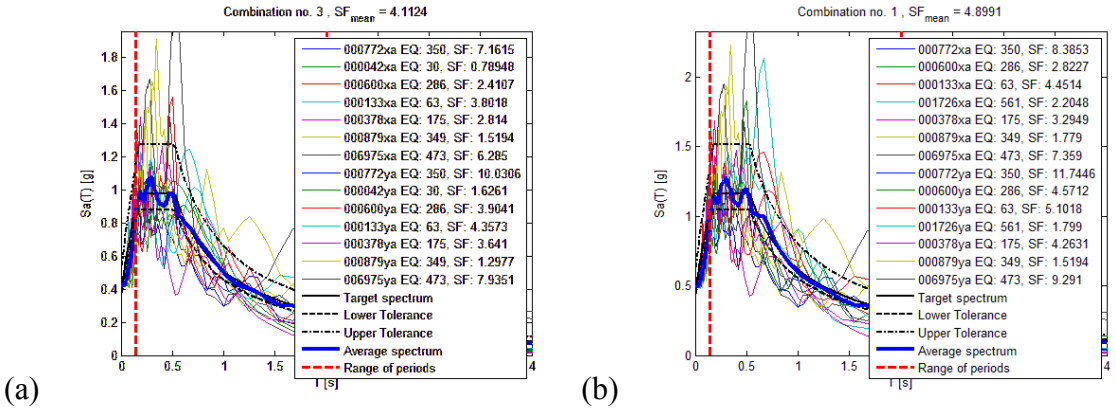

Figure 4: Scaled ground motion spectra and target spectra for LLS (a) and CLS (b).

Waveform ID	PGAx [m/s^2]	PGAz [m/s^2]	Station ID	Earthquake Name	Magnitude Mw	R_{ep} [km]
772	0.5673	0.405	ST223	Umbria Marche (aftershock)	5.3	20
42	5.1459	2.4983	ST8	Ionian	5.8	15
600	1.6852	1.0406	ST223	Umbria Marche	6	22
133	1.0686	0.9324	ST33	Friuli (aftershock)	6	9
378	1.4437	1.1158	ST152	Lazio Abruzzo	5.9	16
879	2.6739	3.1306	ST271	Dinar	6.4	8
6975	0.6464	0.512	ST3272	Izmit (aftershock)	5.8	26

Table 4: Selected natural ground motions for LLS.

Waveform ID	PGAx [m/s^2]	PGAz [m/s^2]	Station ID	Earthquake Name	Magnitude Mw	R_{ep} [km]
772	0.5673	0.405	ST223	Umbria Marche (aftershock)	5.3	20
600	1.6852	1.0406	ST223	Umbria Marche	6	22
133	1.0686	0.9324	ST33	Friuli (aftershock)	6	9
1726	2.1575	2.6442	ST549	Adana	6.3	30
378	1.4437	1.1158	ST152	Lazio Abruzzo	5.9	16
879	2.6739	3.1306	ST271	Dinar	6.4	8
6975	0.6464	0.512	ST3272	Izmit (aftershock)	5.8	26

Table 5: Selected natural ground motions for CLS.

6 RESULTS OF THE NON-LINEAR ANALYSES

Figure 5 shows the comparison between the capacity curve in X-direction of the case-study structure retrofitted with damped braces characterized by $\mu_{DB} = 6$ with the results of BNLDA, expressed as the maximum displacement at the last story and the maximum base shear. In particular, Figure 5(a) shows the results relevant to the accelerograms of LLS, while in Figure 5(b) the results of the CLS analyses are reported. Both the results for the seven bidirectional accelerograms and their average value (labelled as "AVG") are shown. The design requirement at the LLS is met since the retrofitted structure attains by average the target displacement d_p, Figure 5(a). On the other hand, in case of CLS accelerograms the structure experiences displacements 11% greater on average than d_p, Figure 5(b). For sake of brevity the comparison is shown only along X-direction and considering only the case of $\mu_{DB} = 6$, however, similar results were obtained also in Z-direction and for different values of μ_{DB}.

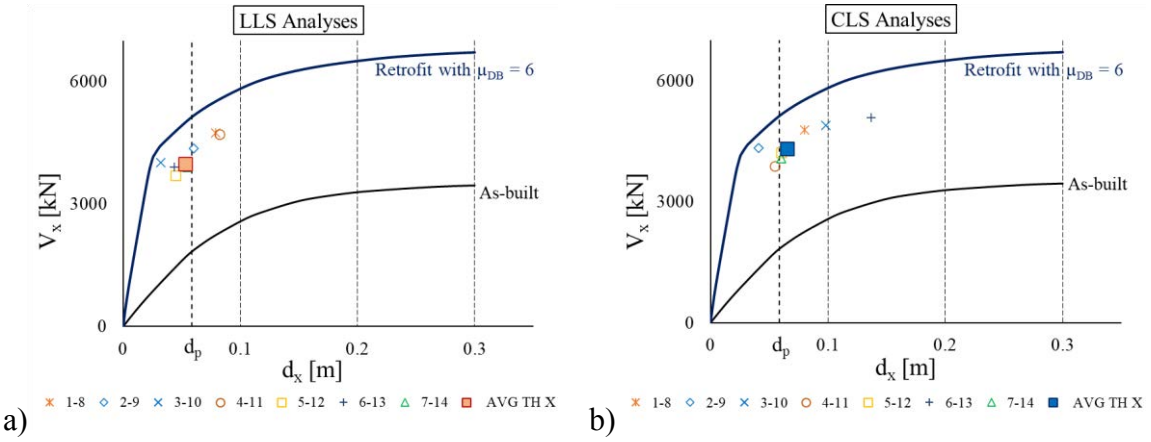

Figure 5: Comparison between the capacity curves of the retrofitted structure with $\mu_{DB} = 6$ and the maximum top displacements versus base shears from BNLDA along X-direction.

The results of the BNLDA were evaluated in terms of maximum displacement (d) and peak acceleration (PFA) at each floor calculated by averaging the maxima of the results obtained for each pair of accelerograms. Figure 6 shows the variation of the maximum top displacement d_{max} and the maximum acceleration among the floors PFA_{max} with respect to the ductility μ_{DB} of the damped brace systems. Increasing μ_{DB} reduces the structural response of the retrofitted building in either limit state condition and along both directions, which is an effect of the larger damping introduced in the structural system by the devices characterized by higher μ_{DB}.

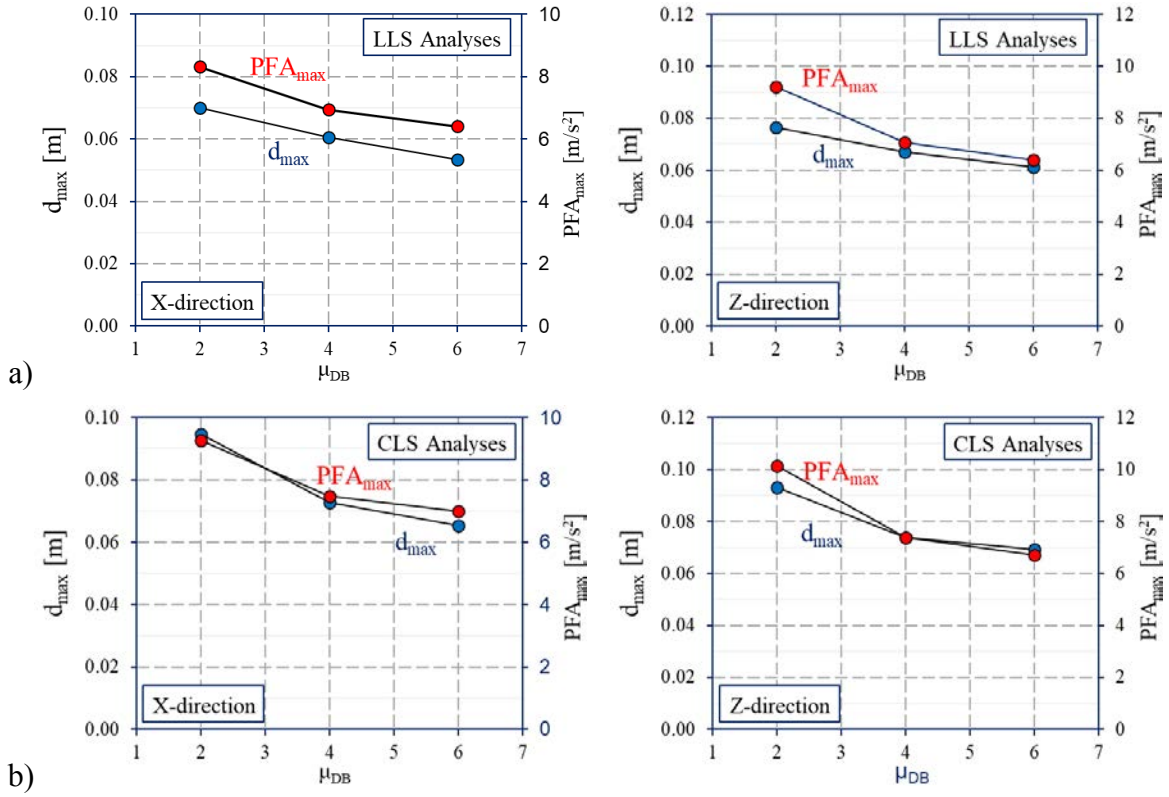

Figure 6: Maximum top displacement d_{max} and peak floor acceleration PFA_{max} along X- and Z- directions for LLS (a) and CLS (b).

The norm EN15129 [26] prescribes that the hysteretic dampers designed for an assigned LLS displacement d_{bd} shall be able to sustain a maximum displacement at CLS of 1.32 d_{bd}. To verify this requirement, the overstroke β between peak damper displacements at CLS and LLS, respectively, was evaluated at each floor and reported in Figure 7, in which the dotted red line corresponds to the limit 1.32 prescribed by the norm [26]. In Z-direction (Figure 7(b)) the ratio β is always lower than the limit, while in X-direction (Figure 7(a)) β at the first floor is greater than 1.32 for every μ_{DB}. It is worth noticing that for $\mu_{DB} = 2$, β exceeds the limit at every floor except at the 5th and 6th floors, while for greater μ_{DB}, the limit is always respected at every floor except the first one.

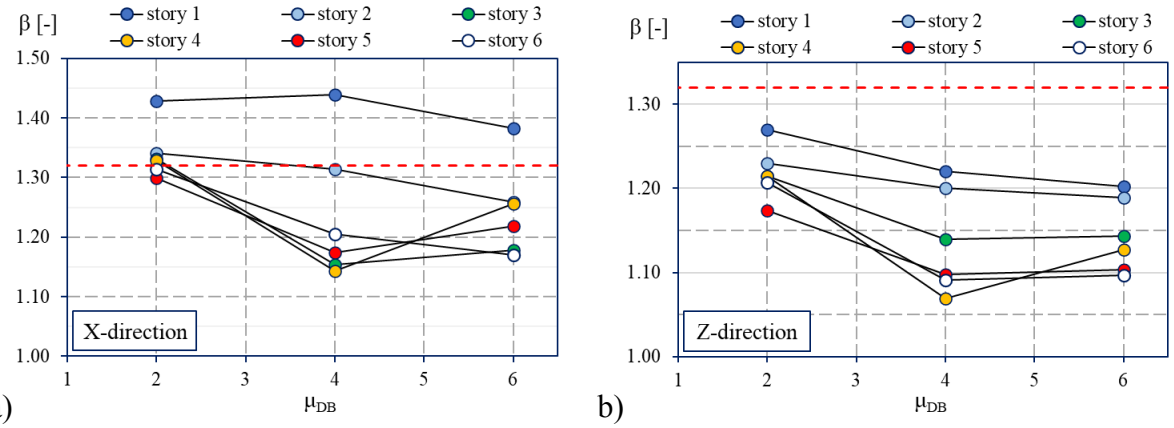

Figure 7: Ratio of the maximum inter-story displacements at CLS and LLS at each floor of the retrofitted structure.

7 CONCLUSIONS

This contribution presents the first results of an ongoing project aimed to investigate the implicit risk associated to structures retrofitted with hysteretic energy dissipation devices subjected to earthquakes of higher intensity than the design seismic scenario.

A case-study RC structure has been investigated and the seismic retrofit has been designed examining three damper solutions, characterized by increasing ductility μ_{DB}. Non-Collapse and Life Safety performance levels have been evaluated through non-linear dynamic analyses performed under bidirectional ground motions considering seven couple of natural earthquakes for each limit state. The results point out that all the energy dissipation systems work effectively under the design earthquake condition, since the retrofitted structure attains on average the target performance. Moreover, higher μ_{DB} values benefit the structure, which undergoes lower displacements and accelerations in both LLS and CLS seismic scenarios.

An important outcome of this work refers to the check of the suitability of the prescription of the European norm EN15129 [26], which requires that the hysteretic devices are able to sustain a larger displacement than their correspondent design seismic displacement d_{bd}, and recommends a limit of 1.32 d_{bd}. The results of the non-linear dynamic analyses have shown that this prescription does not seem appropriate, since all the dampers installed at the first floor in the perimetral X-direction frames of the case-study structure underwent larger displacements than the 1.32 d_{bd} limit. Moreover, in case of $\mu_{DB} = 2$, this limit was never verified expect for the dampers installed at the last two floors.

Even though more cases need to be examined to validate these outcomes, the study provides a first insight to identify critical aspects of the retrofit design and to provide the basis for the computations of the implicit risk of the seismic collapse of retrofitted structures and of local failure of the dampers. The future research will investigate structures with different number of floors (low-, mid- and high-rise buildings) and retrofitted with hysteretic dampers characterized by different ductility values, in order to cover a large range of μ_{DB}.

REFERENCES

[1] V. Quaglini, C. Pettorruso, E. Bruschi, Experimental and numerical assessment of prestressed lead extrusion dampers. *International Journal of Earthquake Engineering*, **XXXVIII**, 46-69, 2021.

[2] V. Quaglini, E. Bruschi, Controllo passivo mediante controventi dissipativi. Principi generali, requisiti normativi ed evoluzione dei principali dispositivi a comportamento dipendente dallo spostamento. *Structural*, **240**, 09. 2022. DOI: 10.12917/STRU240.09.

[3] F.C. Ponzo, A. Di Cesare, A. Telesca, A. Pavese, M. Furinghetti, Advanced modelling and risk analysis of RC buildings with sliding isolation systems designed by the Italian seismic code. *Applied Sciences*, **11**, 1938, 2021. https://doi.org/10.3390/app11041938.

[4] E. Bruschi, V. Quaglini, Assessment of a novel hysteretic friction damper for the seismic retrofit of reinforced concrete frame structures. *Structures*, **46**, 793-811, 2022. DOI: 10.1016/j.istruc.2022.10.113.

[5] E. Bruschi, L. Zoccolini, S. Cattaneo, V. Quaglini, Experimental characterization, modelling and numerical evaluation of a novel friction damper for the seismic upgrade of existing buildings. *Materials*, **16**, 1933, 2023. https://doi.org/10.3390/ma16051933.

[6] J.E. Martínez-Rueda, On the evolution of energy dissipation devices for seismic design. *Earthquake Spectra*, **18(2)**, 309-346, 2002. DOI: 10.1193/1.1494434.

[7] D. Cardone, N. Conte, A. Dall'Asta, A. Di Cesare, A. Flora, N. Lamarucciola, F. Micozzi, F.C. Ponzo, L. Ragni, RINTC-E Project: the seismic risk of existing Italian RC buildings retrofitted with seismic isolation. *7th ECCOMAS Thematic Conference on Computational Methods in Structural Dynamics and Earthquake Engineering*, Crete, Greece, June 24-26 2019.

[8] CSLLPP (Consiglio Superiore dei Lavori Pubblici). D.M. 17 gennaio 2018 in materia di "norme tecniche per le costruzioni". Gazzetta ufficiale n.42 del 20 febbraio 2018, Supplemento ordinario n.8, Ministero delle Infrastrutture e dei trasporti, Roma; 2018, in Italian.

[9] CEN (European Committee for Standardization). Design of structures for earthquake resistance – Part 1: General rules, seismic actions and rules for building. EN 1998–1 Eurocode 8; 2005.

[10] V. Quaglini, C. Pettorruso, E. Bruschi, Design and experimental assessment of a prestressed lead damper with straight shaft for seismic protection of structures. *Geosciences*, **12**, 182, 2022. DOI: 10.3390/geosciences12050182.

[11] V. Quaglini, V. Pettorruso, E. Bruschi, Supplemental energy dissipation with prestressed Lead Extrusion Dampers (P-LED): Experiments and modeling. *8th ECCOMAS Thematic Conference on Computational Methods in Structural Dynamics and Earthquake Engineering*, Athens, Greece, 28–30 June 2021.

[12] V. Quaglini, E. Bruschi, C. Pettorruso, M. Sartori, Design and experimental assessment of a novel damper with high endurance to seismic loads. *Structural Integrity Procedia*, **44(C)**, 1451-1457, 2023. https://doi.org/10.1016/j.prostr.2023.01.186.

[13] A. Di Cesare, F.C. Ponzo, D. Nigro, Assessment of the performance of hysteretic energy dissipation bracing systems. *Bulletin of Earthquake Engineering*, **12(6)**, 2777–2796, 2014. DOI: 10.1007/s10518-014-9623-z.

[14] E. Bruschi, V. Quaglini, Numerical investigation on the seismic performance of a RC framed building equipped with a novel Prestressed LEad Damper with Straight Shaft. *Structural Integrity Procedia*, **44(C)**, 1443-1450, 2023. https://doi.org/10.1016/j.prostr.2023.01.185.

[15] V. Quaglini, E. Gandelli, P. Dubini, M.P. Limongelli, Total displacement of curved surface sliders under nonseismic and seismic actions: A parametric study. *Structural Control and Health Monitoring*, **24(12)**, e2031, 2017. https://doi.org/10.1002/stc.2031.

[16] V. Quaglini, E. Gandelli, P. Dubini, Experimental investigation of the re-centring capability of curved surface sliders. *Structural Control and Health Monitoring*, **24(2)**, e1870, 2016. https://doi.org/10.1002/stc.1870.

[17] E. Gandelli, D. De Domenico, P. Dubini, M. Besio, E. Bruschi, V. Quaglini, Influence of the breakaway friction on the seismic response of buildings isolated with curved surface sliders: Parametric study and design recommendations. *Structures*, **27**, 788-812, 2020. https://doi.org/10.1016/j.istruc.2020.06.035.

[18] E. Gandelli, V. Quaglini, Effect of the static coefficient of friction of curved surface sliders on the response of an isolated building. *Journal of Earthquake Engineering*, **24(9)**, 1361-1389, 2018. https://doi.org/10.1080/13632469.2018.1467353.

[19] E. Gandelli, V. Quaglini, P. Dubini, M.P. Limongelli, S. Capolongo, Seismic isolation retrofit of hospital buildings with focus on non-structural components. *Ingegneria Sismica*, **35(4)**, 20-56, 2018.

[20] D. Cardone, L.R.S. Viggiani, G. Perrone, A. Telesca, A. Di Cesare, F.C. Ponzo, L. Ragni, F. Micozzi, A. Dall'Asta, M. Furinghetti & A. Pavese. Modelling and Seismic Response Analysis of Existing Italian Residential RC Buildings Retrofitted by Seismic Isolation. *Journal of Earthquake Engineering*, **27:4**, 1069-1093, 2023. https://doi.org/10.1080/13632469.2022.2036271.

[21] A. Di Cesare, F.C. Ponzo, A. Telesca, Improving the earthquake resilience of isolated buildings with double concave curved surface sliders. *Engineering Structures*, **228**, 111498, 2021. https://doi.org/10.1016/j.engstruct.2020.111498.

[22] A. Di Cesare, F.C. Ponzo, A. Telesca, Mechanical model of the over-stroke displacement behaviour for double concave surface slider anti-seismic devices. *Frontiers in Built Environment*, **8**, 1083266. https://doi.org/10.3389/fbuil.2022.1083266.

[23] V. Zayas, S. Mahin, M.C. Constantinou, Safe and Unsafe Seismically Isolated Structures. PEER Report No. 20016-01; Pacific Earthquake Engineering Research Center, Berkeley, CA, USA, 2016.

[24] L. Ragni, D. Cardone, N. Conte, A. Dall'Asta, A. Di Cesare, A. Flora, G. Leccese, F. Micozzi, F.C. Ponzo, Modelling and seismic response analysis of Italian code-conforming base-isolated buildings. *Journal of Earthquake Engineering*, **22 (Suppl. 2)**, 198–230, 2018. https://doi.org/10.1080/13632469.2018.1527263.

[25] P. Franchin, F. Noto, Partial factors for displacement-based seismic design and assessment consistent with the second-generation of Eurocodes. *14th International Conference on Applications of Statistics and Probability in Civil Engineering*, ICASP14, Dublin, Ireland, 9-13 July, 2023.

[26] CEN (European Committee for Standardization). European Committee for Standardization (2009). EN 15129. Anti-seismic devices. Brussels.

[27] F. McKenna, G.I. Fenves, M.H. Scott, Open System for Earthquake Engineering Simulation, PEER Report, Berkeley, CA; 2000.

[28] OpenSeesWiki online manual. Available online at: https://opensees.berkeley.edu/wiki/index.php/Main_Page [last access: April 2021].

[29] F. Faleschini, M.A. Zanini, K. Toska, Seismic reliability assessment of code-conforming reinforced concrete buildings made with electric arc furnace slag aggregates, *Engineering Structures*, **195**, 324-339, 2019. DOI: 10.1016/j.engstruct.2019.05.083.

[30] E. Bruschi, P.M. Calvi, V. Quaglini, Concentrated plasticity modelling of RC frames in time-history analyses. *Engineering Structures*, **243**, 112716, 2021. DOI: 10.1016/j.engstruct.2021.112716.

[31] E. Bruschi, V. Quaglini, P.M. Calvi, Numerical assessment of concentrated plasticity models of ductile RC frames in non-linear dynamic analyses. *2nd fib Italy YMG Symposium on Concrete and Concrete Structures*, Rome, Italy, November 18-19, 2021.

[32] M.H. Scott, G.L. Fenves, Plastic Hinge Integration Methods for Force-Based Beam-Column Elements. *Journal of Structural Engineering*, **132(2)**, 244-252, 2006. DOI: 10.1061/(ASCE)0733-9445(2006)132:2(244).

[33] CEN (European Committee for Standardization). Design of structures for earthquake resistance – Part 3: Design of structures for earthquake resistance. EN 1998–3 Eurocode 8; 2005.

[34] M. Menegotto, P.E. Pinto, Method of analysis for cyclically loaded RC plane frames including changes in geometry and non-elastic behaviour of elements under combined normal force and bending. *IABSE: Symposium on resistance and ultimate deformability of structures acted on by well defined repeated loads* 1973 – Final Report.

[35] F.C. Filippou, E.P. Popov, V.V. Bertero. Effects of Bond Deterioration on Hysteretic Behavior of Reinforced Concrete Joints, Report EERC 83-19, *Earthquake Engineering Research Center*, University of California, Berkeley, 1983.

[36] S. Popovics, A numerical approach to the complete stress-strain curve of concrete. *Cement and Concrete Research*, **3(5)**, 583-599, 1973.

[37] F. Barbagallo, M. Bosco, E. Marino, P. Rossi, On the fibre modelling of beams in RC framed buildings with rigid diaphragm. *Bulletin of Earthquake Engineering*, **18**, 189-210, 2020. DOI: 10.1007/s10518-019-00723-z.

[38] S. Mazzoni, F. McKenna, M.H. Scott, G.L. Fenves, B. Jeremic, OpenSEES command language manual. *Pacific Earthquake Engineering Research Center*, University of California, Berkeley, 2003.

[39] E. Bruschi, V. Quaglini, P.M. Calvi, A simplified design procedure for seismic upgrade of frame structures equipped with hysteretic dampers. *Engineering Structures*, **251**, e113504, 2021. DOI: 10.1016/j.engstruct.2021.113504.

[40] V. Quaglini, E. Bruschi, C. Pettorruso, Dimensionamento di dispositivi dissipativi per la riabilitazione sismica di strutture intelaiate. Structural, **e237**, 2021. DOI: 10.12917/STRU237.25.

[41] E. Bruschi, V. Quaglini, P.M. Calvi, A simplified design procedure to improve the seismic performance of RC framed buildings with hysteretic damped braces. *New Metropolitan Perspectives 2022 - 5th International Symposium "Post COVID Dynamics: Green and Digital Transition, between Metropolitan and Return to Villages' Perspectives"*, Reggio Calabria, Italy, 25-27 May 2022, Volume 482 LNNS, pp. 2173 – 2182, ISBN: 978-3-031-06825-6.

[42] E. Bruschi, V. Quaglini, L. Zoccolini, Control of the seismic response of steel-framed buildings by using supplementary energy dissipation devices, *Applied Sciences*, **13(4)**, 2063, 2023. DOI: 10.3390/app13042063.

[43] A. Di Cesare, F.C. Ponzo, Seismic retrofit of reinforced concrete frame buildings with hysteretic bracing systems: design procedure and behaviour factor. *Shock and Vibration*, e2639361, 2017. DOI: 10.1155/2017/2639361.

[44] N. Ambraseys, P. Smit, R. Sigbjornsson, P. Suhadolc, B. Margaris, Internet-Site for European Strong-Motion Data, European Commission, Research-Directorate General, Environment and Climate Programme, 2002.

[45] I. Iervolino, C. Galasso, E. Cosenza, REXEL: computer aided record selection for code-based seismic structural analysis. *Bulletin of Earthquake Engineering*, **8,** 339-362, 2010. https://doi.org/10.1007/s10518-009-9146-1.